1 Weakening the cooling effect of northern peatlands on the global climate

2 system during the 21st century

- 3 Bailu Zhao¹, Qianlai Zhuang^{1,2}
- ⁴ Department of Earth, Atmospheric, and Planetary Sciences, Purdue University, West Lafayette, Indiana,
- 5 47907
- 6 ²Department of Agronomy, Purdue University, West Lafayette, IN 47907
- * Correspondence to: gzhuang@purdue.edu

8 9

Abstract

- 10 Northern peatlands have been a carbon sink since initiation as projected by process-based models.
- 11 However, most existing models are limited by lacking sufficient processes of N cycle. Here we use a
- 12 peatland biogeochemistry model incorporated with N-related processes of fixation, deposition, gas
- 13 emission, loss through water flow, net mineralization, plant uptake and litterfall, to project the role of
- 14 the peatlands in biogeochemical climate forcing. Simulations from 15-ka BP to 2100 are conducted
- driven by CMIP5 climate forcing data of IPSL-CM5A-LR and bcc-csm1-1 and warming scenarios of RCP
- 16 2.6, RCP 4.5 and RCP 8.5. During the Holocene, northern peatlands have an increasing cooling effect
- with radiative forcing (RF) up to -0.57 W·m⁻². By 1990, these peatlands accumulate 408 Pg C and 7.8 Pg
- 18 N. Under warming, increasing mineral N content enhances plant net primary productivity, the cooling
- 19 effect persists. However, RF increases by 0.1-0.5 W·m⁻² during the 21st century, mainly due to the
- stimulated CH₄ emissions. Northern peatlands could switch from a C sink to a source when annual
- 21 temperature exceeds -2.2 -0.5°C. This study highlights the role of N in increasing the peatland cooling
- 22 effect while the enhanced CH₄ emissions counterbalance the effect in future northern peatlands carbon-
- 23 climate feedbacks.

Introduction

24

32

33

34

35

36

37

38 39

40

41

- 25 Peatlands have less than 3% of global land coverage, with most of them in northern high latitudes
- 26 (>45°N) ¹. Despite the low coverage, C storage in northern peatlands is estimated to be 450±100 Pg C
- 27 (Hugelius 2020, Spahni 2013) due to the high C content on unit area. Carbon in northern peatlands is
- 28 stored in soil organic layer, which can be a few meters in depth ³. Soil organic matter accumulates under
- 29 cold and wet conditions, where anoxic environment slows down the rate of dead plant decomposition 4.
- 30 Most of the northern peatlands initiated after 12 ka BP and have been acting as a C sink since their
- 31 initiation ⁵.

In the future, the northern high latitude region is likely to experience more severe warming than the other part of the Earth ⁶. This change in climate may interrupt the long-lasting pattern of C accumulation of northern peatlands. The direct influences of warming include the increase of both productivity and microbial activity (i.e., decomposition rates), indicating more intensive C sequestration and releasing ^{7,8}. Warming also enhances peat decomposition indirectly via drought and permafrost thaw, with the former switches partial soil C from anaerobic to aerobic condition and the latter releases previously-frozen peat for decomposition ^{9,10,11,12}. In addition, fires and human-derived land use change are likely to release significant amount of C into the atmosphere ¹³. Under multiple controlling factors, northern peatlands are projected to be a weaker C sink or switch to a C source by the end of the 21st century ^{14,15,16}.

These projections of northern peatland C balance are made using process-based models such as LPX-Bern 1.0 ¹⁶, ORCHIDEE-PEAT ¹⁷, LPJ-GUESS ¹⁸, HPM ¹⁹ and PTEM 2.2 ¹⁵ (Table 1). However, one common uncertainty source of these models is the lack of a complete nitrogen cycle ^{15, 16, 20}. For example, LPX-Bern 1.0 has included atmospheric N deposition and other N inputs, vegetation N uptake, litter N fall and N mineralization ¹⁶. PTEM 2.2 includes the same processes as LPX-Bern 1.0, and also considers the N loss from water runoff ¹⁵. These models are unable to track nitrification, denitrification, biological N fixation (BNF) and N gas loss, and a mineral N pool is missing. Although a DyN model is developed based on LPJ-DGVM framework (Table 1) and considers these N-related processes missing in current peatland models, DyN is not designed to describe peatland biogeochemical process and was not applied to peatlands simulation ²¹. Notably, higher N availability could increase the productivity of woody plants, reduce that of Sphagnum, and increase the decomposition rate of northern peatlands, and vice versa ^{22, 23, 24}. With the incomplete N cycle, current peatland models are limited in quantifying past and future C budget.

To address this knowledge gap, we embedded a complete N cycle to PTEM 2.2 and create an updated PTEM 2.3 (Fig. 1). The N pool is divided into PFT vegetation N pools, soil organic N pool and mineral N pool. The mineral N pool is composed of three layers following the hydrology module v structure of PTEM 2.2. In each layer, the mineral N pool is further divided into NH₄+, NO₃- and NO₂- pools. There are N fluxes on horizontal direction via mineralization, nitrification, denitrification, run on/run-off and on vertical direction via gravity-driven water flow, vegetation N uptake, N litterfall, gas emission, N fixation and N deposition (Fig. 1). A simulation from 15 ka BP to 2100 is conducted. Since the previous study has indicated less than 0.1MKm² peatland area variation during 1990-2100 ¹⁵, the peatland extent is assumed to be fixed during this period. The following questions are answered: a) how did northern peatlands accumulate C and N during the Holocene (15ka BP-1990)? b) How will northern peatlands C and N fluxes and stocks respond to the future climate change? c) What is the threshold temperature and precipitation for pan-Arctic sink and source shift? d) How are the C and N stocks, fluxes and the thresholds different from the simulation without a complete N cycle?

Results and discussion

Holocene C and N dynamics

The total N stock in northern peatlands is controlled by four N fluxes: N fixation, N deposition, N gas emission and water flow (Fig. 2(a)). In particular, the N flux through BNF, deposition and gas emission are stable through the Holocene, with an average rate of 0.80±0.09 gN·m⁻²·yr⁻¹, 0.69±0.09 gN·m⁻²·yr⁻¹ and 0.24±0.06 gN·m⁻²·yr⁻¹, respectively. On average, the water flow carries more N out than carrying in, and the N lose rate through water flow shows a slightly increase trend until around 6ka BP then stabilized. This indicates the expansion of mineral N pool size at the regional scale and stabilization after around 6ka BP, i.e., the rates of mineral N flowing in and out of the ecosystem are similar since then. The long-term N loss via water flow is 0.91±0.27 gN·m⁻²·yr⁻¹. Although all these N fluxes are inorganic, the input N is mostly converted to and stored as organic matter (both vegetation and soil, Fig. 2(b)). In particular, mineral N is converted into organic N via vegetation N uptake, and the reverse process is the positive net N mineralization (Appendix Fig. 3 (a) & (b)). Since vegetation N uptake rate is generally higher than net N mineralization (1.53±0.20 vs. 1.08±0.28 gN·m⁻²·yr⁻¹), a net conversion from mineral to organic N is simulated. Furthermore, the vegetation N uptake rate and litter N fall rate are close, indicating most of the system input N are transferred from vegetation N pool to soil organic N pool

(Appendix Fig. 3 (c)). A slower accumulation of N is simulated during 8-6 ka BP, which is likely driven by the cooling and drying condition during this period (Appendix Fig. 4).

Although the simulation starts in 15 ka BP, major increases in SOC and SON stocks are not found until 11-12 ka BP (Fig. 2 (c)). By 1990, the northern peatlands soil C stock is 408 Pg, which is close to the estimation from PTEM 2.1 (404 Pg C) ²⁵, Qiu, Zhu ²⁶ (408 Pg C) and Hugelius, Loisel ²⁷ (400 Pg C). The estimated soil organic N stock is 7.8 Pg, within in the range of 10±7 reported by Hugelius, Loisel ²⁷. Since soil N stock is predominantly organic, the C:N ratio can be approximated by the organic C: organic N ratio, which is 52.26. This ratio is slightly lower than the values from Loisel (2014) (52.3 vs. 55±33) and higher than values from Hugelius, Loisel ²⁷ (52.3 vs. 41.5).

The long-term C accumulation rate (CAR) of pan-Arctic peatlands is 23.43 gC·m⁻²·yr⁻¹, which is similar to the estimation from PTEM 2.1 (22.9 gC·m⁻²·yr⁻¹, ²⁵), and agrees with the observed or simulated values from the literature (17.3-26.1 gC·m⁻²·yr⁻¹, ^{2,3,14,28}). The temporal trend of 500-yr CAR from this study is generally consistent with Loisel, Yu ³, Nichols and Peteet ²⁹ and Zhao, Zhuang ²⁵ (Fig. 3). In PTEM 2.1 simulation ²⁵ where a complete N cycle is not considered and the wetland WTD is not derived from TOPMODEL, the simulation result is closer to Loisel, Yu ³. However, in this study, the simulated CAR is closer to Nichols and Peteet ²⁹. The temporal trend of 500-yr NAR is consistent with Loisel, Yu ³, and the long-term NAR is close (0.45 gN·m⁻²·yr⁻¹ vs. 0.5±0.04 gN·m⁻²·yr⁻¹) (Fig. 3(a) & (c)). On a 500-year bin basis, the pan-Arctic peatlands CAR range is 11.40-27.65 gC·m⁻²·yr⁻¹, and the range for NAR is 0.25-0.54 gN·m⁻²·yr⁻¹. The hotspots of C and N accumulations are spatially consistent (Fig. 3(b) & (d)).

As soil C and N accumulates in northern peatlands, the GHG emissions increase simultaneously (Fig. 2 (d) & (e)). Notably, as the mineral N pool size kept increasing and stabilized since around 6ka BP, N₂O emissions showed the same trend. During the Holocene, northern peatlands always act as a C sink and has a net cooling effect on global climate (Fig. 2 (f)). This cooling effect amplifies as more C is sequestrated into soil, which trend is consistent with previous studies ^{30, 31}. In particular, the cooling effect is mainly driven by net ecosystem exchange (i.e., NEE, net CO₂ uptake), with CH₄ emissions have warming effect and N₂O emissions have minor effect (Appendix Fig. 5). Notably, a rapid increase in GHG emission rate is simulated since around 1870 (Appendix Fig. 6). After over 100 years of increasing, by 1990, the regional N₂O, soil heterotrophic respiration (R_H) and CH₄ emissions are 56.30 GgN·yr⁻¹, 327.35 TgC·yr⁻¹ and 47.97 TgC·yr⁻¹, respectively. Due to the increase in GHG emissions, northern peatlands show slightly increased RF which reaches -0.57 W·m⁻² by 1990. This RF value is close to -0.2 - -0.5 W·m⁻² estimated by Frolking and Roulet ³⁰. The discrepancy could be due to the divergent peatland C pool estimates between these models and the differences in impulse-response model parameters used to calculate RF ³¹.

N fluxes, N stocks and the influence on NPP during 1990-2100

As climate warming, all N fluxes are more intensive, with the N loss via water flow increases more than the other pathways (Fig. 4). Despite the limited number and high uncertainties of BNF in northern peatlands ³², our estimated BNF during 2010-2020 (0-2.88 gN·m⁻²·yr⁻¹, with an average of 1.12 gN·m⁻²·yr⁻¹) is close to the observed range during the same period (0.01-3.5 gN·m⁻²·yr⁻¹) ^{33, 34}.

Under the RCP 2.6, northern peatlands are a N sink. Under the RCP 4.5, northern peatlands maintain a N sink with bcc-csm1-1 forcing, and switch from a sink to N neutral with IPSL-CM5A-LR forcing. Under the RCP 8.5, northern peatlands switch from a sink to a N source under both forcing.

Notably, in all scenarios, there is consistently increasing of mineral N stock (Fig. 4, Appendix Table 2). On the contrary, the organic N stock switches from a sink to nearly N neutral under the RCP 2.6, and switches to a source under the RCP 4.5 and RCP 8.5. This is the result of the overall higher increase in net N mineralization than vegetation N uptake (Appendix Fig. 10, Fig. 4). Similar to this study, an increase in net N mineralization rate is reported under higher temperature ³⁵. Therefore, peat soil is generally mineralized under warming. In particular, during 2000-2100, the organic N stock increases by 0.1 Pg N under the RCP 2.6, 0-0.1 Pg N under the RCP 4.5, and decreases by 0.1-0.2 Pg N under the RCP 8.5. In addition, the warmer, lower latitude regions first show organic N loss (Appendix Fig. 11 & 12). However, the mineral N stock keeps increasing under all warming scenarios by 0.1, 0.1-0.2 and 0.2-0.3 Pg N under the RCP 2.6, RCP 4.5 and RCP 8.5, respectively (Appendix Table 2, Appendix Fig. 13). As a result, the total N pool increases by 0.1-0.2 Pg N under all scenarios, with hotspots in eastern Eurasia and arctic North America (Appendix Fig. 14 & 15).

Our estimation of recent N_2O emissions is supported by the literature. In particular, during 2009-2013, observations of N_2O emissions have a range of 0-3.1 gN·m⁻² ^{36, 37}, while our estimated N_2O emission rate is 0-2.88 gN·m⁻²·yr⁻¹. At regional scales, N_2O emission is estimated to be 30-100 Gg N·yr⁻¹ in the early 1990s, while our estimate is 58.63-61.35 Gg N·yr⁻¹ during the same period ³⁸. Previous study suggests that warming alone has limited effect on N_2O emissions in boreal peatlands, while more abundant mineral N content could increase N_2O emissions ³⁹. Similarly, N_2O emissions are reported to peak after N fertilization in Swedish bogs ⁴⁰. In addition, permafrost thaw (i.e. reduced permafrost area and deepening ALD, Appendix Fig. 7-9, Appendix Table 2) is simulated during warming, leading to a high amount of N taking part in nitrification and denitrification, and benefits N_2O emissions ⁴¹. Under these effects, we estimate that during the 21st century, N_2O emission increases by 30.5-37.4, 48.6-95.7 and 189.3-277.8 Gg N·yr⁻¹ under the RCP 2.6, RCP 4.5 and RCP 8.5, respectively (Appendix Table 2, Appendix Fig. 13). However, the contribution of N_2O emissions to future warming is minor due to the relatively small amount (Appendix Fig. 21), which agrees with Hugelius, Loisel ²⁷.

With the warmer climate and higher mineral N content, the vegetation N uptake increases and thereby stimulating NPP (Fig. 4, Appendix Fig. 16). In particular, compared with previous simulation with no complete N cycle, this study projects higher NPP in the future ¹⁵. The correlation coefficient (R²) between N uptake and NPP is 0.45-0.84, depending on the warming scenario (Fig. 4). During 2000-2100, regional NPP increases by 12-33.6, 57.7-62.9 and 86.5-100.1 TgC·yr⁻¹ under the RCP 2.6, RCP 4.5 and RCP 8.5, respectively (Appendix Table 2).

C fluxes, C stocks and the radiative forcing during 1990-2100

As C sequestration increases, the C emissions are also more intense (Fig. 5). From 2000-2100, under the RCP 2.6, RCP 4.5 and RCP 8.5, R_H increase by 38.9-59.5, 71.0-160.6 and 281.4-351.4 TgC·yr⁻¹, respectively, while the increase of CH₄ emissions is 8.9-11.7, 19.0-42.2 and 101.5-142.3 TgC·yr⁻¹, respectively (Appendix Table 2). The increase in CO₂ emissions is a result of higher temperature and PFT shift. In particular, the expansion of woody plants is simulated by PTEM 2.2 as WTD drawdown in the 21st century (Zhao 2023), and the woody plants are more susceptible to decomposition. An indirect effect of more abundant N is that higher NPP stimulates CH₄ emissions ⁴². Compared with the simulation without a complete N cycle ¹⁵, the CH₄ emissions by 2100 is higher in this study by 12.8-68.0 TgC·yr⁻¹. Notably, the increase in CH₄ emissions is not solely due to higher productivity, but also driven by the effect of WTD dynamics and temperature increase. Previous simulation indicates that northern

peatlands WTD will be deeper during the 21st century, which has a negative effect on CH₄ emissions $^{15, 43}$. However, our results indicate that the positive effects of warming and NPP will override the negative effect of deeper WTD and thereby CH₄ emissions still increase.

With more NPP increase than C emissions, northern peatlands maintain as a C sink until at least 2100 under the RCP 2.6 with both forcing and the RCP 4.5 with bcc-csm1-1 forcing. The opposite trend is found under the other three warming scenarios (i.e., IPSL-CM5A-LR + RCP 4.5, IPSL-CM5A-LR + RCP 8.5 and bcc-csm1-1 + RCP 8.5), where northern peatlands become a C source of 2.7, 10.3 and 2.7 Pg C, respectively (Fig. 5, Appendix Table 2). This projection agrees with the result from Qiu, Zhu ⁴⁴. Under all scenarios, warmer climate (i.e., higher temperature and precipitation) correlates with less C sink capability of pan-Arctic peatlands (Table 2). Therefore, as temperature increases, CAR generally decreases, with the warmer, lower latitude regions first switch to C sources (Appendix Fig. 17 & 18). Similarly, Chaudhary, Westermann ¹⁴ estimate lower CAR as temperature increases, while the northern peatlands are still C sinks until 2100 under the RCP 8.5 in their study.

Compared with the simulation without N cycle (Zhao 2023), with both forcings, the CAR in the 21st century is consistently higher in the simulation with N cycle (Appendix Fig. 19 & 20). In particular, in the higher altitude, the CAR with N cycle is higher, while the opposite is found in the lower latitude region. Since the region with higher peatland abundance tends to have higher CAR with N cycle, the N cycle increases regional average CAR by 2.5-16.3 gC·m⁻²·yr⁻¹. As climate warms up in the late 21st century, the delta CAR becomes higher, indicating the increasing importance of N cycle under future warming in C cycling (Appendix Fig. 19 & 20).

We estimate that with 1°C annual temperature increase, the northern peatlands C sink capability decreases by 14.6-48.9 TgC·yr⁻¹, and the correlation is better when warming is severe (Table 2). With 1mm annual precipitation increase, the northern peatlands C sink capability decreases by 0.4-3.8 TgC·yr⁻¹. However, this does not prove that higher precipitation suppresses C sink capacity of northern peatlands. Instead, the negative correlation between precipitation and C sink capacity is more likely to be a result of the temperature rise co-existing with precipitation increase. The comparison between IPSL-C5A-LR and bcc-cam1-1 can support this argument. To date, with 1°C annual temperature increase, the precipitation under IPSL-CM5A-LR increases less than under bcc-csm1-1, while the opposite is found in C sink capacity (Table 2). This indicates peatland C sink capacity prefers highmoisture conditions, while the increase in moisture cannot offset the negative effect of higher temperature.

Threshold temperature, precipitation and unfrozen day number corresponding to the C sink to source conversion of northern peatlands are calculated, while relatively high R² values exist only when persistent sink to source conversion happens (i.e., IPSL-CM5A-LR + RCP 4.5, IPSL-CM5A-LR + RCP 8.5 and bcc-csm1-1 + RCP 8.5). Under these three scenarios, when calculating only from forcing and model output during the 21st century, the threshold temperature is -2.2 - -0.5°C, the threshold precipitation is 487.2-507.6 mm·yr⁻¹, and the threshold unfrozen day number is 193-213 (Table 2). When calculating from the long-term forcing and model output during 15ka BP-2100, the threshold is similar to a temperature of -2.2 - -0.1°C, and precipitation of 487.2-524.4 mm·yr⁻¹ (Appendix Table 3). Compared with previous simulation with no complete N cycle, this study projects higher threshold temperature determining northern peatlands C sink-source conversion (-2.2 - -0.5°C vs. -2.9 - -2.1°C), and the projected conversion is delayed ¹⁵.

Under all scenarios, the RF of northern peatlands remains negative, indicating a cooling effect persists despite the warming (Fig. 5). However, the RF under all scenarios increases, suggesting a weaker cooling effect in the future. Under all scenarios, the RF derived from CO₂ flux is stable and N₂O emissions has minor effects on the total RF (Appendix Fig. 21, Appendix Table 4). Therefore, the increase of RF is mainly driven by higher emissions of CH₄, which has a shorter lifetime ⁴⁵ and responds to climate change swiftly (Appendix Fig. 21). In particular, the RF derived from CH₄ emissions contribute to 93%-100% of RF increase during 2000-2050, and 90-99% of RF increase during 2050-2100 (Appendix Table 4). In agreement to this study, Qiu, Ciais ¹⁷ projects an increased warming effect from CH₄ emissions during 1990-2100. Similarly, Hugelius, Loisel ²⁷ suggests that under warming and permafrost thaw, the main driver of GHG forcing is CH₄ emissions. At site level, CH₄ emissions account for 60-85% of the total CO₂ equivalent emissions in a drained coastal wetland ⁴⁶. During 2000-2100, the northern peatlands RF increases by 0.1, 0.1-0.2 and 0.3-0.5 W·m⁻² under the RCP 2.6, RCP 4.5 and RCP 8.5, respectively (Appendix Table 2), indicating there is a positive feedback between northern peatlands and future warming.

Methods

PTEM overview and model revisions

PTEM 2.2 is a version of Terrestrial Ecosystem Model (TEM) incorporated with biogeochemical processes of northern peatlands. PTEM 2.2 run simulation on monthly time step, and there are four PFTs considered: moss, herbaceous, shrub and trees ¹⁵. In each month, the C sequestrated by the ecosystem is allocated into four PFTs according to their relevant dominance, which is influenced by WTD, N availability and the PFT's current plant C. In addition, the productivity of moss is also influenced negatively by the coverage of vascular plants due to the shadowing effect ⁴². In each month, a PFT-specific fraction of plant C and N falls as litter and become inputs to soil organic C and N pools. The soil C pool is divided into 1cm layers and the bulk density, C density, fraction of remaining original litter and C content of each layer are calculated.

PTEM 2.2 simulates both aerobic and anaerobic decomposition. In particular, when the soil layer is not saturated, the decomposition is aerobic and produces CO₂, otherwise the decomposition is mainly anaerobic and produces limited amount of CO₂ but mostly CH₄. PTEM 2.2 has a soil thermal module keeping track of the ALD. When the soil layer is frozen, there is no decomposition ⁴². Different from soil C, soil organic N pool in PTEM 2.2 is not divided into layers, but exists as a whole. The plant-available N comes from rainfall, run on and net N mineralization, while available N loss pathways are vegetation N uptake and N outflow ⁴². In particular, the net N mineralization rate is influenced by the soil C:N ratio and the intensity of microbial activity (surrogated by soil C decomposition rate).

PTEM 2.2 simulation is composed of two steps: WTD simulation and peat simulation. In WTD simulation, PTEM 2.2 estimates the WTD of the entire grid cell (0.5°×0.5°). The output WTD is interpolated into 100 sub-grid cell bins by TOPMODEL, such that the dynamic WTD in each bin can be estimated and used as the input for peat simulation. In peat simulation, the WTD input is used for four purposes: 1) determining the boundary of aerobic and anaerobic decomposition; 2) estimating soil moisture; 3) calculating run off and baseflow; 4) when the precipitation alone is not sufficient to maintain the input WTD, additional run on will be added. By influencing run on and runoff, WTD input is indirectly used in the N cycle ¹⁵.

The N cycle influences C cycle in PTEM with two key carbon fluxes: NPP and decomposition. In each month, NPP is the highest when not limited by N availability, which is affected by the C:N ratio of plants. When plant C:N ratio reaches maximum, there is no sufficient N to support additional C assimilation thereby NPP is the lowest, and vice versa. The C:N ratio is not only determined by the C and N amount in the existing plant tissue, but also the amount of N uptake by the plants in the current month. Therefore, even if the C:N ratio in the existing plant tissue reaches maximum, the plants can still assimilate C by additional N uptake. The rate of plant N uptake is influenced by the amount of available mineral N. In terms of decomposition, PTEM has PFT-specific decomposition parameters. These parameters are influenced by the C:N ratio of the litter, i.e., plant C:N ratio by the end of the growing season. When N is insufficient and the ratio is higher, there is a lower decomposition rate. In this study, PTEM 2.2 is revised into PTEM 2.3 by adding the N cycle (Fig. 1). The details of model revision is provided in Appendix Text 1.

Same as PTEM 2.1 (Zhao 2022 (b)), PTEM 2.3 requires spatially-explicit peat initiation input. The peat thickness, soil organic C stock and soil organic N stock all start as 0 in the year of peat initiation. An equilibrium run is conducted before transient simulation, while no spin up period is used. This is because the model variables usually stabilize after decades of simulation, which is very short compared with the total simulation period (usually thousands of years). Compared with previous versions, the revised PTEM 2.3 can estimate a) the pool size of plant available N based on better understanding of various N pools and fluxes, b) NPP and decomposition based on the revised N availability, and c) N_2O emissions such that the whole budget of peatland GHG emissions can be derived. Different from Forest-DNDC which has been used for wetland GHG emission estimation (Li 2005), PTEM 2.3 does not consider disturbances such as drainage or management practices. In addition, both DNDC and TRIPLEX-GHG have microbial biomass in C pools and keep track of nitrifiers and denitrifiers in the N pools (Zhang 2017). PTEM 2.3 has simplified processes without these pools. However, as a model designed for peatlands, PTEM has moss as a PFT, and keeps track of the peat thickness and the relative position of water table.

Model simulation and post-processing

The model is parameterized in terms of the C:N ratio determining the balance between mineralization and immobilization, and the spatially-explicit monthly maximum C assimilated by the ecosystem. The parameterization method is provided in Appendix Text 2. The historical model input (15ka BP-1990) is derived from TraCE 21ka dataset ⁴⁷ and the future inputs are derived from two CMIP5 products: IPSL-CM5A-LR and bcc-csm1-1, covering three warming scenarios: RCP 2.6, RCP 4.5 and RCP 8.5. Both datasets were selected partially because they both cover until at least 2100, and they have three warming scenarios. Among many CMIP5 data products, IPSL-CM5A-LR dataset has low biases compared with the historical data in Eurasia and North America (Miao 2014, Sheffield 2013). However, IPSL-CM5A-LR predicts extreme warming in RCP 8.5, thereby bcc-csm1-1 dataset was also selected as a milder projection. A simulation was conducted with both forcings by PTEM 2.2, which has not implemented the N cycle. Therefore, in this study, we use the same forcing on a revised PTEM 2.3, such that the role of N cycle can be analyzed by comparing the two simulations. Both historical and two CMIP5 forcings are corrected by CRU dataset. The processing of historical and future model inputs is documented in Appendix Text 3. The correction of CMIP5 forcing makes sure that the difference of future C and N dynamics is derived from the different levels of warming in the future, but not the

difference of these forcings in the past. In order to simulate the C and N dynamics of northern peatlands during 15 ka BP-2100, three sets of simulations were conducted:

- 1) WTD simulation: PTEM 2.3 is first used to simulate the WTD of each grid cell from 15 ka BP-2100. In particular, this simulation is conducted for six times as there are two sets of future CMIP5 forcing and three warming scenarios. The simulated grid cell WTD is used to estimate the dynamic wetland WTD with TOPMODEL.
- 2) Preliminary PTEM 2.3 simulation: the wetland WTD derived from step 1 is used as an input to this simulation. This simulation is conduced only once for the past (15 ka BP-1990). The output spatially-explicit peat thickness is used to establish the spatially-explicit peat expansion trend with the method in Zhao, Zhuang ²⁵.
- 3) Final PTEM 2.3 simulation: the spatially-explicit peat expansion trend from step 2 and wetland WTD from step 1 are both inputs to this simulation. This simulation is conducted six times covering 15ka BP-2100. No future peat expansion/shrinkage is considered.

The simulation results of step 3 are analyzed in terms of 1) historical C and N accumulation and greenhouse gas (GHG) emission; 2) future organic and mineral N dynamics and their impact on C dynamics; 3) future GHG emissions and C budget; 4) the threshold temperature and precipitation determining the northern peatlands C sink/source conversion. The threshold temperature and precipitation are calculated with the same method as PTEM 2.2 simulation ¹⁵. In particular, Table 2 provides the threshold calculated from forcing data and model outputs during 1990-2100, while appendix Table 3 provides the result from long-term forcing and outputs, i.e., 15ka BP-2100.

The radiative forcing (RF) of peatlands GHG fluxes is calculated to evaluate the effect of northern peatlands on climate. The estimation of RF is derived from the impulse-response model designed for peatlands ³¹. This model divides CO₂ fluxes into five pools by their lifetime, and CH₄ fluxes is treated as a whole pool. The atmospheric perturbation due to GHG flux is calculated by the annual net GHG emission, the lifetime of GHG in each pool and the fraction of each pool in total flux. In addition, in order to convert from atmospheric perturbation to RF, the GHG's radiative efficiency (W·m⁻²·ppb⁻¹), an indirect multiplier of GHG and the converter between GHG emissions (Tg) to ppb is required. These parameters are given for the CO₂ and CH₄ pools, but not N₂O pool ³¹. Therefore, we assume N₂O to be an entire pool, with the lifetime of 121 years and radiative efficiency of 3×10⁻³ W·m⁻²·ppb⁻¹ ⁴⁵. The indirect effect multiplier is 1 since the indirect effects has large uncertainties ⁴⁵. The unit converter is 7.65 Tg N₂O per ppb, as derived from Denman, Brasseur ⁴⁸.

Acknowledgments

323 This study is financially supported by an NSF project (#1802832).

Data access

The model codes and output data used in this manuscript can be accessed in Purdue University Research Repository (https://purr.purdue.edu/publications/4241/1).

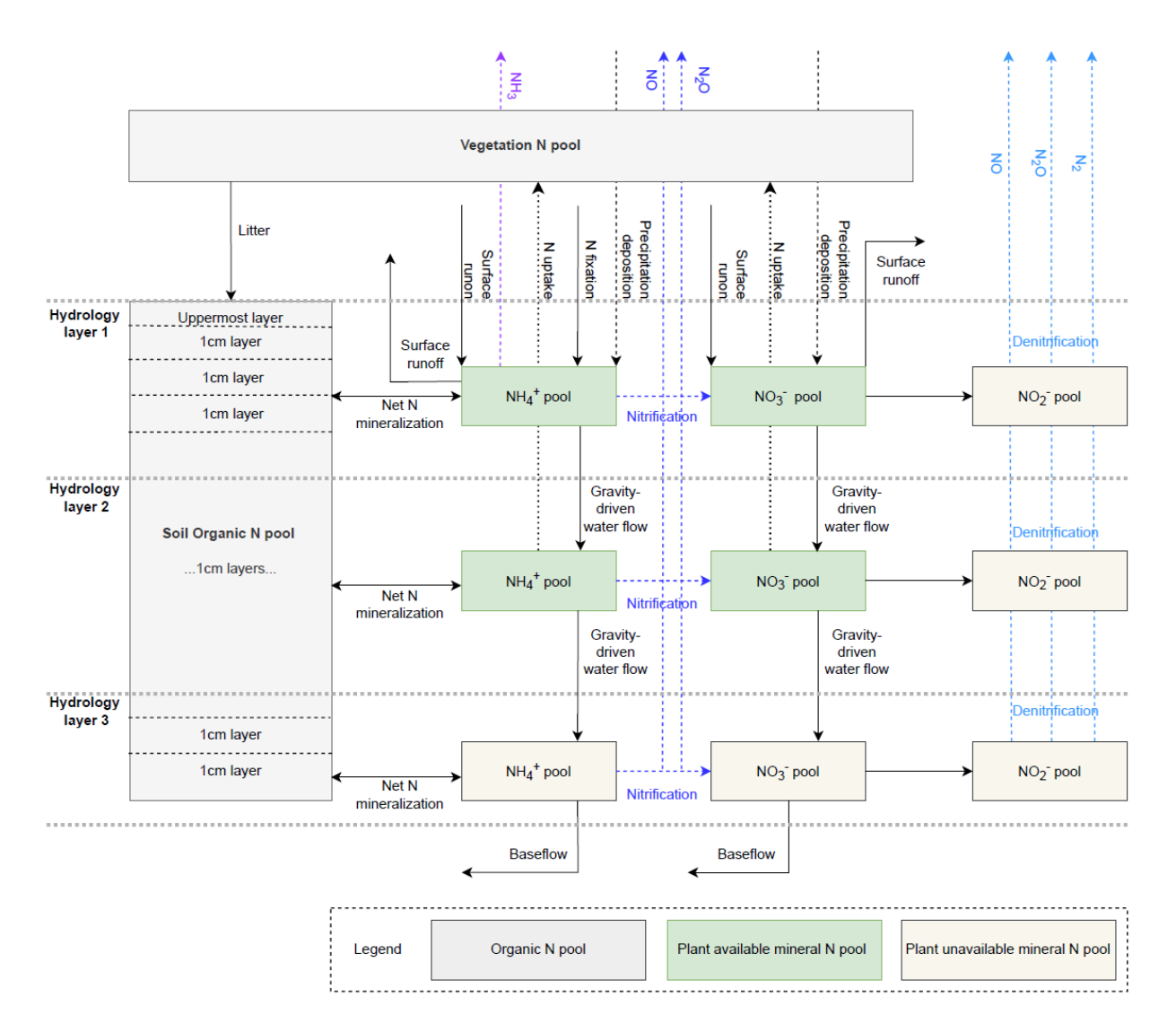


Fig. 1. The N cycle in PTEM 2.3.

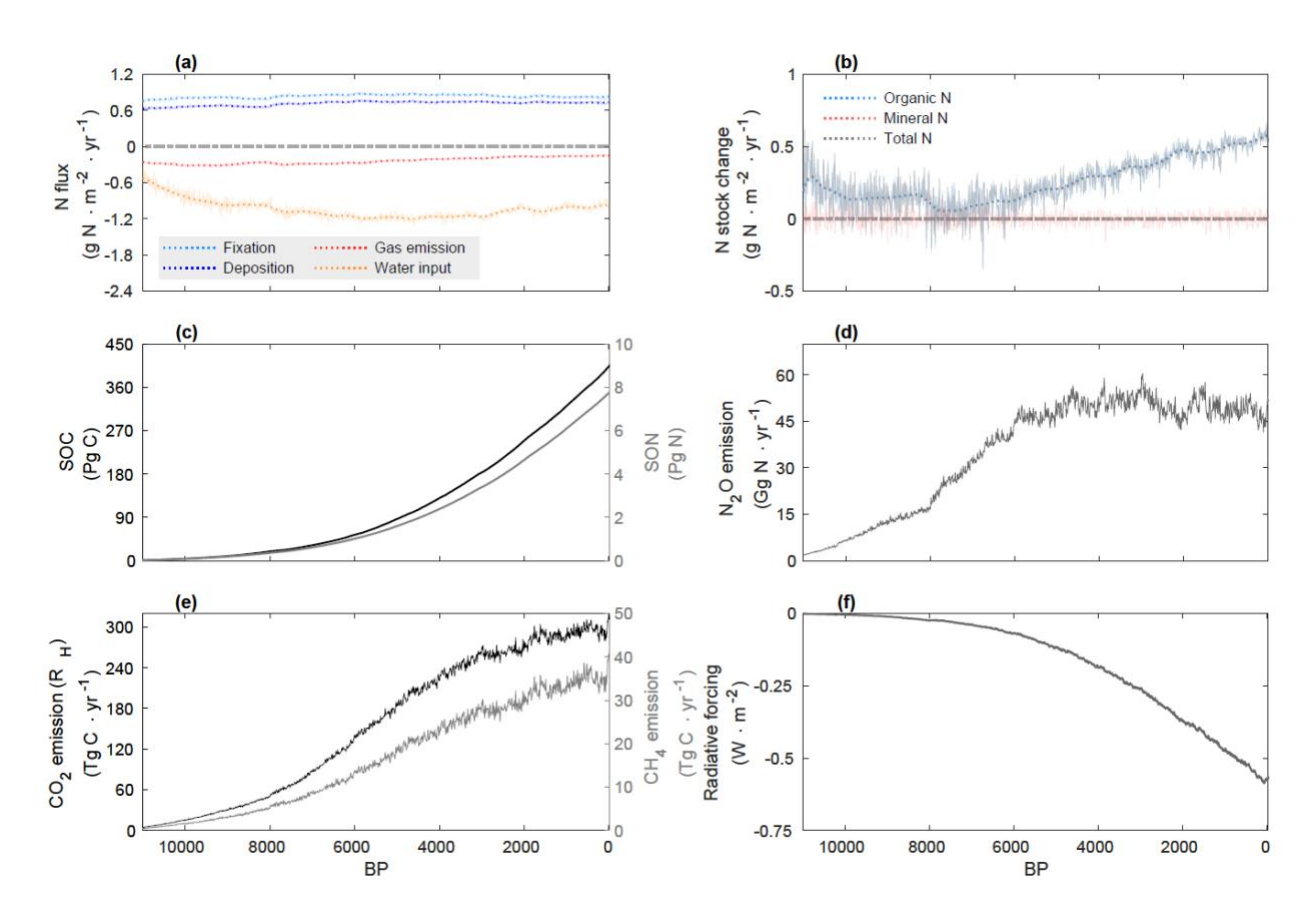


Fig. 2. The time series of (a) N fluxes through BNF, deposition, gas emission and water flow; (b) changes in organic, mineral and total N stock; (c) soil organic C and organic N stock; (d) regional N₂O emission; (e) regional soil heterotrophic respiration (R_H) and CH₄ emission; (f) the radiative forcing of northern peatlands.

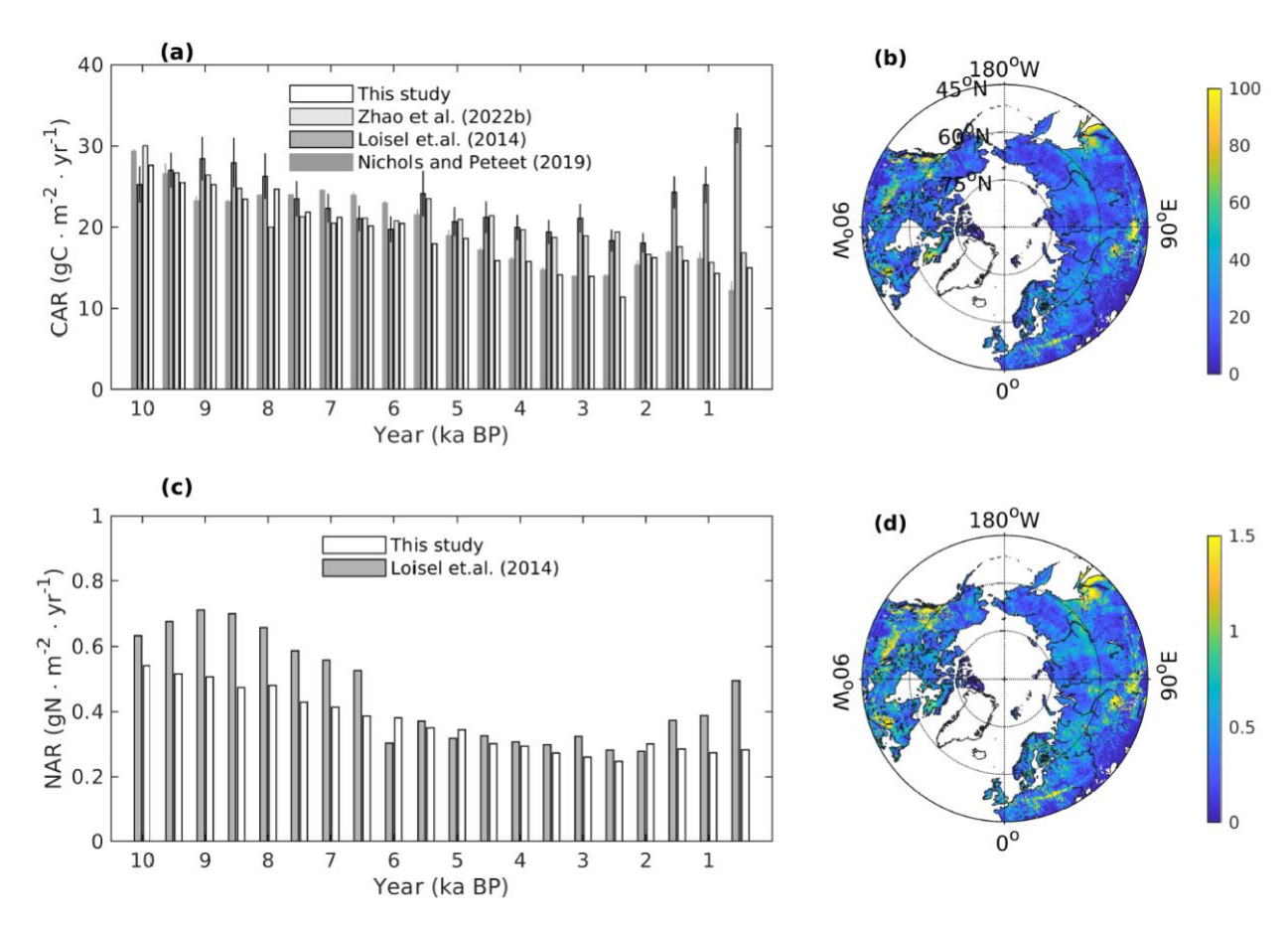


Fig. 3. (a) Comparison of 500-yr CAR between this study and Loisel, Yu ³, Nichols and Peteet ²⁹ and Zhao, Zhuang ²⁵. (b) Spatially-explicit long-term CAR. (c) Comparison of 500-yr NAR between this study and Loisel, Yu ³. (b) Spatially-explicit long-term NAR.

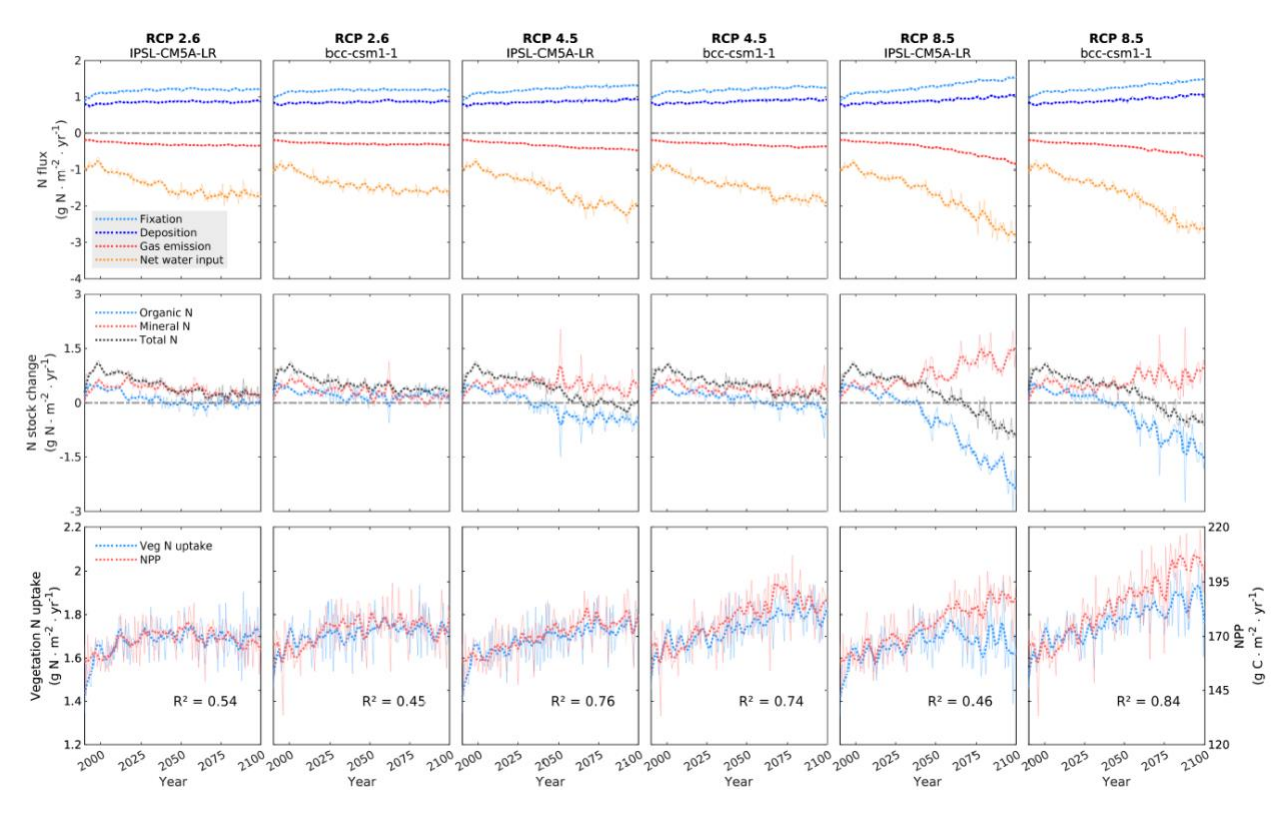


Fig. 4. Time series of N fluxes (top panel), changes in organic and mineral N stocks (middle panel) and vegetation N uptake and NPP (bottom panel) during 1990-2100.

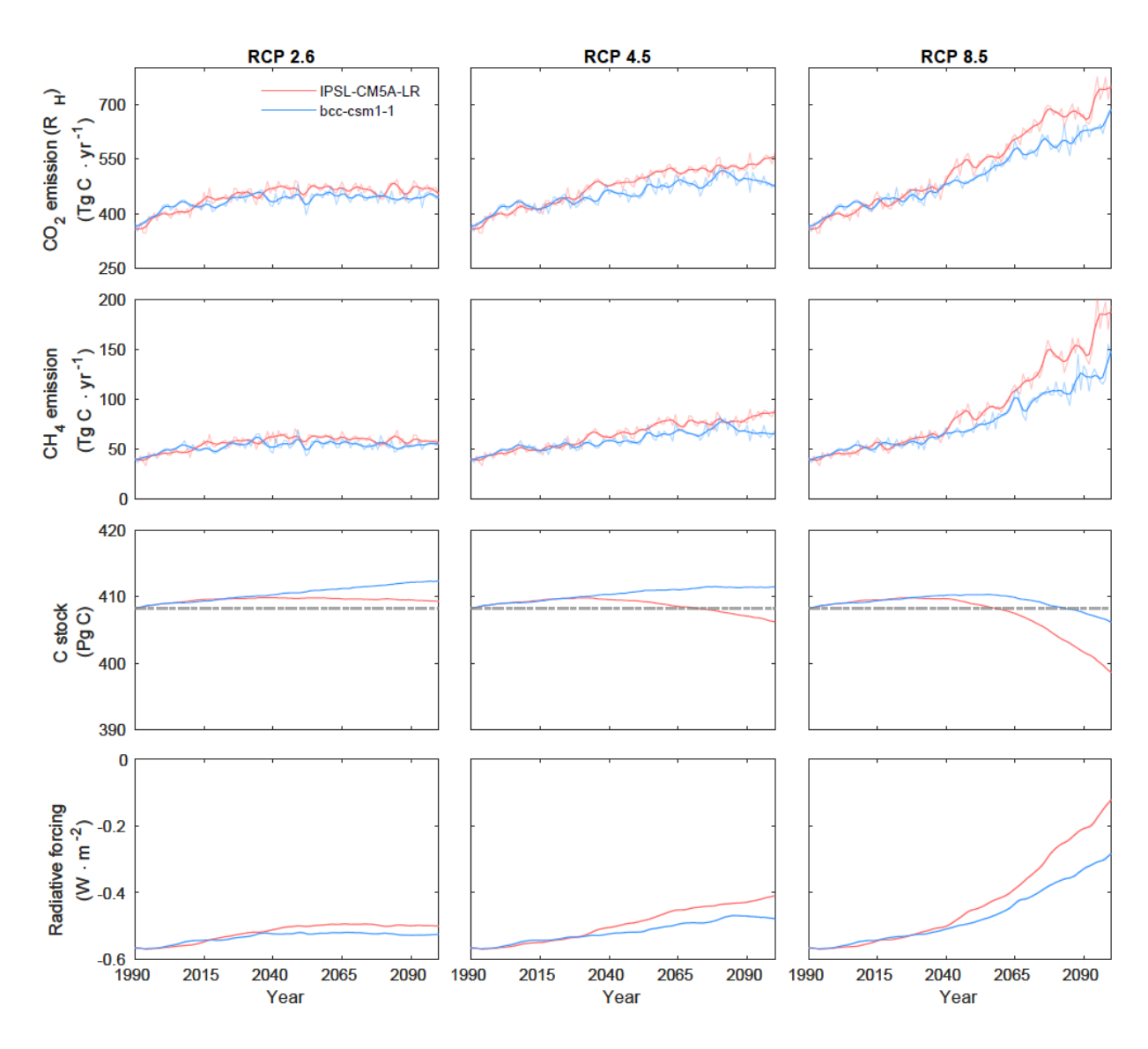


Fig. 5. Time series of soil heterotrophic respiration (R_H), CH_4 emissions, C stock and RF of northern peatlands during 1990-2100.

Table 1. List of abbreviations

Abbreviation	Full name
LPX-Bern	Land surface Processes and eXchanges model Bern version
	•
ORCHIDEE-PEAT	Organising Carbon and Hydrology In Dynamic Ecosystems, peatland version
LPJ-GUESS	Lund-Potsdam-Jena General Ecosystem Simulator
HPM	Holocene Peatland Model
PTEM	Peatland Terrestrial Ecosystem Model
TEM	Terrestrial Ecosystem Model
DyN	The global Dynamic Nitrogen model
DNDC	DeNitrification DeComposition
LPJ-DGVM	Lund-Potsdam-Jena Model Dynamic Global Vegetation Model
PFT	Plant Functional Type
WTD	Water Table Depth
ALD	Active Layer Depth
BNF	Biological N Fixation
TWI	Topographic Wetness Index
GHG	Greenhouse Gas
CAR	C Accumulation rate
NAR	N accumulation rate
RF	Radiative Forcing
R_{H}	Soil heterotrophic respiration
NPP	Net Primary Productivity
NEE	Net Ecosystem Exchange

 Table 2. Pan-Arctic peatlands C sink capability and its sensitivity to climate

Model	RCP 2.6	R^2	RCP 4.5	R^2	RCP 8.5	R ²	
	Pan-Arctic	peatlands C	sink capability in	creases (Tg (C·yr⁻¹) in respons	se to 1°C annual	
	temperature increase						
IPSL-CM5A-LR	-28.2	0.53	-34.6	0.76	-48.9	0.92	
bcc-csm1-1	-18.1	0.13	-14.6	0.18	-32.5	0.76	
	Pan-Arctic peatlands C sink capability increases (Tg C·yr ⁻¹) in response to 1mm annual						
	precipitati	on increase					
IPSL-CM5A-LR	-1.4	0.38	-2.1	0.61	-3.8	0.87	
bcc-csm1-1	-0.4	0.02	-0.7	0.13	-2.1	0.68	
	Annual temperature threshold of C sink-source conversion						
IPSL-CM5A-LR	-1.8	0.19	-2.2	0.71	-2.0	0.67	
bcc-csm1-1	4.4	0.01	0.6	0.08	-0.5	0.60	
	Annual precipitation threshold of C sink-source conversion						
IPSL-CM5A-LR	496.5	0.16	487.2	0.57	490.4	0.64	
bcc-csm1-1	682.8	0.00	529.3	0.13	507.6	0.58	
	Annual un	frozen day th	reshold of C sinl	k-source conv	version		
IPSL-CM5A-LR	192	0.62	193	0.89	211	0.76	
bcc-csm1-1	_*	_*	219	0.50	213	0.87	
	Annual precipitation increase (mm) in response to 1°C annual temperature increase						
IPSL-CM5A-LR	12.7	0.58	13.3	0.82	12.0	0.92	
bcc-csm1-1	13.4	0.37	14.3	0.66	13.6	0.89	

^{*} An effective threshold can not be identified.

358	References			
359 360	1.	Xu J, Morris PJ, Liu J, Holden J. PEATMAP: Refining estimates of global peatland distribution based on a meta-analysis. <i>CATENA</i> 2018, 160 : 134-140.		
361 362 363 364	2.	Turunen J, Tomppo E, Tolonen K, Reinikainen A. Estimating carbon accumulation rates of undrained mires in Finland–application to boreal and subarctic regions. <i>The Holocene</i> 2002, 12 (1): 69-80.		
365 366 367 368	3.	Loisel J, Yu Z, Beilman DW, Camill P, Alm J, Amesbury MJ, et al. A database and synthesis of northern peatland soil properties and Holocene carbon and nitrogen accumulation. <i>The Holocene</i> 2014, 24 (9): 1028-1042.		
369 370 371 372	4.	Finlayson CM, Milton GR. Peatlands. In: Finlayson CM, Milton GR, Prentice RC, Davidson NC (eds). <i>The Wetland Book: II: Distribution, Description, and Conservation</i> . Springer Netherlands: Dordrecht, 2018, pp 227-244.		
373 374 375 376	5.	Gorham E, Lehman C, Dyke A, Janssens J, Dyke L. Temporal and spatial aspects of peatland initiation following deglaciation in North America. <i>Quaternary Science Reviews</i> 2007, 26 (3): 300-311.		
377 378 379	6.	GISTEMP-Team. GISS Surface Temperature Analysis (GISTEMP), version 4, NASA Goddard Institute for Space Studies. 2021.		
380 381 382 383	7.	Richardson AD, Hufkens K, Milliman T, Aubrecht DM, Furze ME, Seyednasrollah B, et al. Ecosystem warming extends vegetation activity but heightens vulnerability to cold temperatures. <i>Nature</i> 2018, 560 (7718): 368-371.		
384 385 386	8.	Hanson PJ, Griffiths NA, Iversen CM, Norby RJ, Sebestyen SD, Phillips JR, et al. Rapid Net Carbon Loss From a Whole-Ecosystem Warmed Peatland. <i>AGU Advances</i> 2020, 1 (3): e2020AV000163.		
387 388 389	9.	Frolking S, Talbot J, Jones MC, Treat CC, Kauffman JB, Tuittila E-S, et al. Peatlands in the Earth's 21st century climate system. <i>Environmental Reviews</i> 2011, 19 (NA): 371-396.		
390 391 392 393	10.	Finger Higgens RA, Chipman JW, Lutz DA, Culler LE, Virginia RA, Ogden LA. Changing Lake Dynamics Indicate a Drier Arctic in Western Greenland. <i>Journal of Geophysical Research: Biogeosciences</i> 2019, 124 (4): 870-883.		
394 395 396	11.	Huang Y, Ciais P, Luo Y, Zhu D, Wang Y, Qiu C, et al. Tradeoff of CO2 and CH4 emissions from global peatlands under water-table drawdown. <i>Nature Climate Change</i> 2021, 11 (7): 618-622.		

398 12. Gallego-Sala AV, Charman DJ, Brewer S, Page SE, Prentice IC, Friedlingstein P, et al. Latitudinal 399 limits to the predicted increase of the peatland carbon sink with warming. Nature Climate 400 Change 2018, 8(10): 907-913. 401 402 13. Loisel J, Gallego-Sala AV, Amesbury MJ, Magnan G, Anshari G, Beilman DW, et al. Expert 403 assessment of future vulnerability of the global peatland carbon sink. Nature Climate Change 404 2021, **11**(1): 70-77. 405 406 14. Chaudhary N, Westermann S, Lamba S, Shurpali N, Sannel ABK, Schurgers G, et al. Modelling 407 past and future peatland carbon dynamics across the pan-Arctic. Global Change Biology 2020, 408 **n/a**(n/a). 409 410 15. Zhao B, Zhuang Q. Peatlands and their carbon dynamics in northern high latitudes from 1990 to 411 2300: a process-based biogeochemistry model analysis. *Biogeosciences* 2023, **20**: 251-270. 412 413 16. Spahni R, Joos F, Stocker BD, Steinacher M, Yu ZC. Transient simulations of the carbon and 414 nitrogen dynamics in northern peatlands: from the Last Glacial Maximum to the 21st century. 415 Clim Past 2013, **9**(3): 1287-1308. 416 417 17. Qiu C, Ciais P, Zhu D, Guenet B, Peng S, Petrescu AMR, et al. Large historical carbon emissions 418 from cultivated northern peatlands. Science Advances 2021, 7(23): eabf1332. 419 420 18. Chaudhary N, Miller PA, Smith B. Modelling past, present and future peatland carbon 421 accumulation across the pan-Arctic region. Biogeosciences 2017, 14(18): 4023-4044. 422 423 19. Treat CC, Jones MC, Alder J, Sannel ABK, Camill P, Frolking S. Predicted Vulnerability of Carbon in 424 Permafrost Peatlands with Future Climate Change and Permafrost Thaw in Western Canada. 425 Journal of Geophysical Research: Biogeosciences 2021, n/a(n/a): e2020JG005872. 426 427 20. Frolking S, Roulet NT, Tuittila E, Bubier JL, Quillet A, Talbot J, et al. A new model of Holocene 428 peatland net primary production, decomposition, water balance, and peat accumulation. Earth 429 Syst Dynam 2010, 1(1): 1-21. 430 431 21. Xu RI, Prentice IC. Terrestrial nitrogen cycle simulation with a dynamic global vegetation model. 432 Global Change Biology 2008, **14**(8): 1745-1764. 433 434 22. Gunnarsson U, Rydin H. Nitrogen fertilization reduces Sphagnum production in bog 435 communities. New Phytologist 2000, 147(3): 527-537.

437 438 439	23.	Ojanen P, Penttilä T, Tolvanen A, Hotanen J-P, Saarimaa M, Nousiainen H, et al. Long-term effect of fertilization on the greenhouse gas exchange of low-productive peatland forests. Forest Ecology and Management 2019, 432 : 786-798.
440 441 442 443	24.	Song Y, Song C, Ren J, Tan W, Jin S, Jiang L. Influence of nitrogen additions on litter decomposition, nutrient dynamics, and enzymatic activity of two plant species in a peatland in Northeast China. <i>Science of The Total Environment</i> 2018, 625 : 640-646.
444 445 446 447	25.	Zhao B, Zhuang Q, Frolking S. Modeling Carbon Accumulation and Permafrost Dynamics of Northern Peatlands Since the Holocene. <i>Journal of Geophysical Research: Biogeosciences</i> 2022, 127 (11): e2022JG007009.
448 449 450 451	26.	Qiu C, Zhu D, Ciais P, Guenet B, Peng S, Krinner G, et al. Modelling northern peatland area and carbon dynamics since the Holocene with the ORCHIDEE-PEAT land surface model (SVN r5488). Geosci Model Dev 2019, 12 (7): 2961-2982.
452 453 454 455	27.	Hugelius G, Loisel J, Chadburn S, Jackson RB, Jones M, MacDonald G, et al. Large stocks of peatland carbon and nitrogen are vulnerable to permafrost thaw. <i>Proceedings of the National Academy of Sciences</i> 2020, 117 (34): 20438.
456 457 458 459	28.	Yu Z, Beilman D, Jones M. Sensitivity of Northern Peatland Carbon Dynamics to Holocene Climate Change. <i>Washington DC American Geophysical Union Geophysical Monograph Series</i> 2009, 184: 55-69.
460 461 462	29.	Nichols JE, Peteet DM. Rapid expansion of northern peatlands and doubled estimate of carbon storage. <i>Nature Geoscience</i> 2019, 12 (11): 917-921.
463 464 465	30.	Frolking S, Roulet NT. Holocene radiative forcing impact of northern peatland carbon accumulation and methane emissions. <i>Global Change Biology</i> 2007, 13 (5): 1079-1088.
466 467 468 469	31.	Dommain R, Frolking S, Jeltsch-Thömmes A, Joos F, Couwenberg J, Glaser PH. A radiative forcing analysis of tropical peatlands before and after their conversion to agricultural plantations. <i>Global Change Biology</i> 2018, 24 (11): 5518-5533.
470 471 472	32.	Yin T, Feng M, Qiu C, Peng S. Biological Nitrogen Fixation and Nitrogen Accumulation in Peatlands. <i>Frontiers in Earth Science</i> 2022, 10 .
473 474 475	33.	van den Elzen E, Bengtsson F, Fritz C, Rydin H, Lamers LPM. Variation in symbiotic N2 fixation rates among Sphagnum mosses. <i>PLOS ONE</i> 2020, 15 (2): e0228383.
476		

477 34. Patova EN, Sivkov MD, Goncharova NN, Shubina TP. Associations between nitrogen-fixing 478 cyanobacteria and sphagnum mosses in floodplain bogs of the middle taiga (European 479 Northeast). Theoretical and Applied Ecology 2020. 480 481 35. Keuper F, van Bodegom PM, Dorrepaal E, Weedon JT, van Hal J, van Logtestijn RSP, et al. A 482 frozen feast: thawing permafrost increases plant-available nitrogen in subarctic peatlands. 483 Global Change Biology 2012, 18(6): 1998-2007. 484 485 36. Dinsmore KJ, Skiba UM, Billett MF, Rees RM, Drewer J. Spatial and temporal variability in CH4 486 and N2O fluxes from a Scottish ombrotrophic peatland: Implications for modelling and up-487 scaling. Soil Biology and Biochemistry 2009, 41(6): 1315-1323. 488 489 37. Audet J, Elsgaard L, Kjaergaard C, Larsen SE, Hoffmann CC. Greenhouse gas emissions from a 490 Danish riparian wetland before and after restoration. Ecological Engineering 2013, 57: 170-182. 491 492 38. Martikainen PJ, Nykänen H, Crill P, Silvola J. Effect of a lowered water table on nitrous oxide 493 fluxes from northern peatlands. Nature 1993, 366(6450): 51-53. 494 495 39. Gong Y, Wu J, Vogt J, Le TB. Warming reduces the increase in N2O emission under nitrogen 496 fertilization in a boreal peatland. Science of The Total Environment 2019, 664: 72-78. 497 498 40. Lund M, Christensen TR, Mastepanov M, Lindroth A, Ström L. Effects of N and P fertilization on 499 the greenhouse gas exchange in two northern peatlands with contrasting N deposition rates. 500 Biogeosciences 2009, 6(10): 2135-2144. 501 502 Voigt C, Marushchak ME, Abbott BW, Biasi C, Elberling B, Siciliano SD, et al. Nitrous oxide 41. 503 emissions from permafrost-affected soils. Nature Reviews Earth & Environment 2020, 1(8): 420-504 434. 505 506 42. Zhao B, Zhuang Q, Treat C, Frolking S. A Model Intercomparison Analysis for Controls on C 507 Accumulation in North American Peatlands. Journal of Geophysical Research: Biogeosciences 508 2022, **127**(5): e2021JG006762. 509 510 43. Evans CD, Peacock M, Baird AJ, Artz RRE, Burden A, Callaghan N, et al. Overriding water table 511 control on managed peatland greenhouse gas emissions. *Nature* 2021, **593**(7860): 548-552. 512 513 44. Qiu C, Zhu D, Ciais P, Guenet B, Peng S. The role of northern peatlands in the global carbon cycle 514 for the 21st century. Global Ecology and Biogeography 2020, 29(5): 956-973. 515 516 45. Myhre G, Shindell D, Bréon F-M, Collins W, Fuglestvedt J, Huang J, et al. Anthropogenic and 517 Natural Radiative Forcing. In: Climate Change 2013: The Physical Science Basis. Contribution of

518 Working Group I to the Fifth Assessment Report of the Intergovernmental Panel on Climate 519 Change. Cambridge, United Kingdom and New York, NY, USA: Cambridge University Press; 2013. 520 521 46. Gatland JR, Santos IR, Maher DT, Duncan TM, Erler DV. Carbon dioxide and methane emissions 522 from an artificially drained coastal wetland during a flood: Implications for wetland global 523 warming potential. Journal of Geophysical Research: Biogeosciences 2014, 119(8): 1698-1716. 524 525 47. He F. SIMULATING TRANSIENT CLIMATE EVOLUTION OF THE LAST DEGLACIATION WITH CCSM3. 526 Doctor of Philosophy thesis, UNIVERSITY OF WISCONSIN-MADISON, Madison, 2011. 527 528 48. Denman KL, Brasseur G, Chidthaisong A, Ciais P, Cox PM, Dickinson RE, et al. Couplings Between 529 Changes in the Climate System and Biogeochemistry. In: Solomon S, Qin D, Manning M, Chen Z, 530 Marquis M, Averyt KB, et al. (eds). Climate Change 2007: The Physical Science Basis. Contribution of Working Group I to the Fourth Assessment Report of the Intergovernmental Panel on Climate 531 532 Change: Cambridge University Press, Cambridge, United Kingdom and New York, NY, USA, 2007. 533 534